7. ACTIVE GALACTIC NUCLEI

https://doi.org/10.1017/S0252921100086152 Published online by Cambridge University Press

Physical Processes in Active Galactic Nuclei

Roland Svensson
NORDITA, Blegdamsvej 17
DK-2100 Copenhagen Ø, Denmark

Abstract

Active galactic nuclei (AGNs) emit continuum radiation evenly spread over up to ten decades in frequency from the radio into the gamma-ray range. Plausible emission mechanisms and their characteristics are reviewed. In the deep potential wells around black holes the mean energy per proton can reach 100 MeV. Part or all of this energy may be channeled to all electrons equally (thermal plasma) or, preferentially, into only a small fraction of the electrons (nonthermal plasma). In the former case thermal Comptonization of soft photons may be the dominant emission mechanism, while in the latter case the synchrotron and the inverse Compton scattering process (synchro-self-Compton) are likely to dominate.

When the compactness parameter $L(h\nu \approx mc^2)/R$ (power L, radius R) exceeds about 10^{30} ergs $cm^{-1} s^{-1}$ or $L > L_c \equiv 10^{30} R$ ergs s^{-1}, then electron-positron pair production takes place due to photon-photon interactions causing the source to shroud itself with an electron-positron atmosphere. The efficiency of pair cascades in converting injected energy into electron-positron rest mass can reach levels of about 10% in static pair atmospheres. The emerging radiation is strongly modified by the pair atmosphere causing the spectrum to soften and to have characteristic breaks.

For emission coming from a region near the Schwarzschild radius, $L > 10^{-3} L_{Edd}$ is sufficient to cause prolific pair production. Radiation pressure then drives a mildly relativistic pair wind with Compton drag limiting the Lorentz factor to be less then 10. The pair rest mass power is at most of the order of L_c.

Most results so far on static pair atmospheres and pair winds are either qualitative or based on simple analytical models. Needed numerical treatments of both time dependent and steady radiative transfer of both the continuum and the annihilation line radiation in mildly relativistic flows are relevant not only for AGNs but also for gamma ray bursts and galactic black hole sources.

1. Introduction

Active galactic nuclei (AGNs) are among the most luminous and compact objects in the universe. They are compact in the sense that their compactness, i.e. their luminosity to size ratio, is large. The luminosity is most likely gravitational in origin with a massive black hole supplying the necessarily deep and compact potential well in which the energy can be released. The gravity of the black hole drives gaseous bulk motions, the kinetic energy of which gets dissipated through e.g. shocks or magnetic reconnection. The dissipated energy is channeled either to heat the bulk of the (thermal) matter or to heat only a small

https://doi.org/10.1017/S0252921100086152 Published online by Cambridge University Press

fraction of the particles to relativistic (nonthermal) energies. The heated matter cools, emitting radiation that before it reaches external observers may affect the bulk motions of the emitting gas (radiation hydrodynamics). Recent reviews covering most aspects of black hole models for AGNs are [1]-[3]. Here (see also [4]) the emphasis will be upon the physical processes responsible for emitting the radiation and for turning a fraction of this radiation into matter in a form (electron-positron pairs) very susceptible to radiation pressure. The environment in which this conversion takes place may either be predominantly thermal or non-thermal. The properties of thermal and nonthermal pair production are reviewed preceded by brief summaries of the continuum emission from AGNs (focusing upon the X-ray emission relevant for pair production), the conditions in black hole models, and the basic radiation mechanisms.

2. The Continuum Radiation from AGNs

The features of the continuum spectra from AGNs relevant for this review are:

(i) The power emitted per logarithmic frequency interval (i.e. νL_ν, with L_ν being the spectral luminosity) is approximately constant over some ten decades in frequency ranging from the IR to the hard X-ray region (see e.g. Fig. I.2 in [3]).

(ii) The shape is not a pure power law with spectral index $\alpha \approx 1$ (where $L_\nu \propto \nu^{-\alpha}$) but has breaks and humps. In particular, νL_ν is in many cases rising towards the unobserved regions in the far IR, the far UV, and the soft γ-rays. Most of the, presently, undetermined bolometric luminosity may arise in these spectral regions.

(iii) The soft X-ray spectral index, α_x, seems to be 'universal' in the sense that α_x for most observed AGNs (Seyfert 1's, narrow emission line galaxies) cluster tightly around a value of 0.7 (e.g.[5]). Similar conclusions are made for the subset of objects studied up to 100 keV or more [6]. QSOs on the other hand do not show a universal power law slope, but have α_x ranging from 0.6 to 1.5 with a mean slope of 1 [7],[8]. When $\alpha<1$ most of the high frequency luminosity emerges at the photon energy where the spectrum has the necessary turnover. The turnover may possibly have been observed at a few MeV for NGC 4151 and MCG 8-11-11 [9],[10] and must occur in the MeV-range for 3C273 [11].

(iv) The general trend for the variability time scale is to decrease with frequency being with few exceptions a day or longer in the X-rays [12],[13]. This indicates that the X-rays may be emitted closest to the region of the primary energy release, while the spectrum at smaller frequencies may be primary energy that has been reprocessed at large distances from the black hole.

(v) Lower limits on the compactness L_ν/R in AGNs ranges from 10^{26} to 10^{29} erg s^{-1} cm^{-1} [14] using the light travel time distance $R \approx c\Delta t$ to get an upper limit on the size.

(vi) The small optical polarization (<2%) in most AGNs and QSOs shows that either the optical emission originates from a thermal process or, if nonthermal, the radiation has been reprocessed. The X-ray polarization is unfortunately not yet known.

3. Black Hole Models for AGNs

Black hole models for AGNs are reviewed in [1]-[3]. The following aspects are important when cosidering pair production in such models:

(i) The size, R, of the emitting gas should be larger than about $3R_s = 6GM/c^2 \approx 10^{14} M_8$ cm, where R_s is the Schwarzschild radius, and M_8 is the black hole mass in units of $10^8 M_\odot$.

(ii) The luminosity, L_1 is limited by the Eddington luminosity $L_E = 2\pi m_p c^3 R_s/\sigma_T \approx 10^{46} M_8$ erg s^{-1}, at which the gravitational force on the protons in an ionized hydrogen gas is balanced by the radiation pressure on the free electrons. In a pure electron-positron gas the Eddington

https://doi.org/10.1017/S0252921100086152 Published online by Cambridge University Press

limit is a factor m_p/m_e smaller, $L_{E,pair} \approx 7\times10^{42} M_8$ erg s^{-1}.

(iii) The compactness L/R is less than $L_E/3R_s \approx 10^{32}$ erg $s^{-1}cm^{-1}$ for gravitationally bound pair free plasmas. The compactness is a parameter of crucial importance in compact hot gases and it is often written in dimensionless form

$$\ell \equiv \frac{L}{R}\frac{\sigma_T}{m_e c^3} = \frac{2\pi}{3}\frac{m_p}{m_e}\left(\frac{L}{L_E}\right)\left(\frac{3R_s}{R}\right), \qquad (1)$$

which interchangeably will be referred to as the compactness or as the luminosity (implying constant size). The maximum Eddington limited value of ℓ is $(2\pi/3)(m_p/m_e) \approx 4000$. In physical units

$$\frac{L}{R} = 4\times10^{28}\ell \text{ erg } s^{-1}cm^{-1}. \qquad (2)$$

(iv) Particle acceleration in the vicinity of a black hole in an electric field typically of the order of the equipartion Eddington magnetic field $B_E \equiv (L_E/R_s^2 c)^{\frac{1}{2}}$ is limited by the Compton drag on the radiation field giving a maximum Lorentz factor $\gamma_{drag} \approx (m_e R_s/m_p r_e)^{1/4} = 4\times10^5 M_8^{1/4}$ [3], r_e being the electron radius.

(v) The temperature of virialized matter at a distance r from the black hole is $T \approx 0.1(m_p c^2/k)(R_s/r) \approx 10^{12}(R_s/r)$K. Thermal electrons (and positrons) at the virial temperature are relativistic ($kT > m_e c^2$) for $r < 10^3 R_s$.

(vi) The condition that photons above pair production threshold produce electron-positron pairs before escaping is approximately that the dimensionless compactness should be larger than unity $\ell > 1$ (see §4).

The two conditions for ample electron-positron pair production in the vicinity of black holes are easily satisfied: First, photons above the threshold energy, mc^2, must be emitted. This is naturally the case in nonthermal mechanisms and occurs in thermal plasmas when $kT > mc^2$. Second, the photons must produce pairs demanding $\ell > 1$, which is satisfied for $L > 10^{-3} L_E$ if the radiation source is at a few Schwarzschild radii.

The locations of pair producing hot plasmas within the standard accretion scenarios are (with increasing accretion rate):

(1) The geometrically thick hot two-temperature ion torus containing ions at the virial temperature and mildly relativistic electrons.

(2) The corona of the standard geometrically thin cool accretion disk.

(3) The corona of the geometrically thick cool radiation torus.

Energy may also be released nonthermally throughout these regions, as well as in any (anisotropic) outflow seen in some and expected in most objects.

4. Physical Processes in AGNs

4.1. Radiation Processes

The physical processes responsible for the continuum emission from AGNs and QSOs are not known although several mechanisms has been suggested. It is likely that different mechanisms operating in spatially separated locations are responsible for the emission in different spectral regions. Only three basic processes are normally involved (1) bremsstrahlung, (2) synchrotron radiation, and (3) Compton scattering [15]. The aspects that varies between different models for the continuum radiation are e.g. (i) the choice of the particle energy distribution (either prescribed or solved for selfconsistently), (ii) the possible escape of particles (before cooling), (iii) the possible supply of external photons with energies much smaller than those of the particles, (iv) the choice of scattering optical depth, and (v) the choice of the spatial distribution of the emitting particles. This incomplete list will certainly

https://doi.org/10.1017/S0252921100086152 Published online by Cambridge University Press

expand.

Some relevant properties of the three basic processes are summarized.

4.1.1. Bremsstrahlung

Electrons or positrons decelerating in the field of charged particles emit radiation with spectral index $\alpha \approx$ a few tenths extending up to the energy of the particle. Only recently were the bremsstrahlung spectra from thermal mildly relativistic plasmas calculated ([16] and references therein). Bremsstrahlung is, however, a very inefficient cooling process. To have a compactness ℓ greater than unity in a mildly relativistic plasma cloud requires a Thomson scattering optical depth larger than unity making Comptonization of soft bremsstrahlung photons to be the dominant cooling process. When Comptonization is important, other sources (e.g. the thermal cyclotron/synchrotron process or external black body photons) often dominate bremsstrahlung as soft photon producers.

4.1.2 Cyclotron/Synchrotron Radiation

Cyclotron/synchrotron radiation is generally an important cooling mechanism and/or soft photon producer as soon as the particles are mildly relativistic. For mildly relativistic thermal equipartion sources in the vicinity of black holes the radiation is heavily selfabsorbed and only the very high harmonics radiated by a few relativistic particles way out in the Maxwellian tail are available as soft photons. This makes the calculated soft photon production rate (and cooling) highly uncertain as deviations from a Maxwellian are very likely in the high energy tail.

Relativistic particles with $\gamma < \gamma_{drag}$ in magnetic fields of order B_E produces synchrotron radiation ranging from the selfabsorption turnover frequency typically in the near IR up to a photon energy of $m_e c^2/\alpha_f$ (independent of B_E) α_f being the fine structure constant [3],[17]. Thus, the synchrotron process could in principle operate even in the X-ray regime.

4.1.3 Compton Scattering

Compton scatterings occur in a variety of forms, thermally and nonthermally, upscattering and downscattering.

Comptonization (upscattering) of low energy (soft) photons in thermal plasmas produces power law spectra (for certain combinations of the Thomson scattering optical depth τ and the temperature $\theta \equiv kT/m_e c^2$) extending up to kT at which energy there is an exponential turnover. The analytical theory at nonrelativistic temperatures ($\theta << 1$) is well developed ([18] for $\tau > 1$, [19] for $\tau < 1$). The smooth nonrelativistic spectrum with logarithmic slope $\alpha \approx (9/2 + \theta^{-1}\tau^{-2})^{\frac{1}{2}} - 3/2$ (for $\tau > 1$) turns into a bumpy spectrum (due to discretness effects) at relativistic temperatures with a slope $\alpha \approx \log(2/\tau)/\log(16\theta^2)$ [20]. Somewhat more complex expressions valid at all temperatures and for spectral slopes of interest in AGNs are found in [21]. Detailed emerging Comptonized spectra at kT > a few tenths of mc^2 have only been calculated numerically [20],[22],[23].

Down-scattering by cold thermal particles are effective at photon energies, where the total relative energy change (during the diffusive escape of the photon) $\Delta\varepsilon/\varepsilon \approx -\varepsilon\tau^2$ is larger than unity, or, eqivalently, for $\varepsilon > 1/\tau^2$. The spectrum emerging from a cold homogeneous cloud, where a power law photon spectrum is uniformly injected, steepens at $\varepsilon_{break} \approx 1/\tau^2$ from the injected spectral index α to $\alpha + \frac{1}{2}$ [18]. The more concentrated the photon injection is towards the center of the cloud, the steeper the spectrum above ε_{break} becomes. Downscattering is fully ef-

https://doi.org/10.1017/S0252921100086152 Published online by Cambridge University Press

fective for particles cold enough ($\theta<<1/\tau^2$). Compton upscattering is then negligible as the Compton parameter $y=4\theta\tau^2<<1$.

Relativistic particles scatter photons of initial energy ε to a final energy $\min(\gamma^2\varepsilon,\gamma)$. Thus, in the Klein-Nishina limit ($\gamma\varepsilon>1$) the Compton scattered spectrum extends up to the energy of the particle ($<\gamma_{drag}mc^2$). A power law distribution of particles $N(\gamma)\propto\gamma^{-p}$ with number index p scatter soft photons into a power law with slope $\alpha=(p-1)/2$. The Compton cooling time of a relativistic particle is $t_{cool}\approx(R/c)\gamma^{-1}\ell^{-1}$, which means that for compactnesses greater than unity particles cool before they escape ($t_{esc}\approx R/c$). To avoid a pileup of cool particles reacceleration (or annihilation if the particles are pairs) is necessary.

4.2. Some Models for the X-Ray Continuum

Models for the X-ray continuum are listed and discussed in [3] and [24]. The three more likely mechanisms put forward to explain the observed X-ray index $\alpha\approx0.7$ are (i) unsaturated thermal Comptonization, (ii) nonthermal Compton upscattering of soft photons and (iii) the synchrotron-self-Compton mechanism.

4.2.1. Thermal Comptonization

Thermal Comptonization of soft photons produces a power law extending up to the thermal energy of the particles. The observed spectral index, $\alpha\approx0.7$, requires that the Compton parameter $y=4\theta\tau^2\approx1$ at nonrelativistic temperatures and there is a similar requirement at relativistic temperatures. As the cooling drastically increases when y increases from being $\lesssim1$ to becoming 10 or so, there is a large range of luminosities for which a source would have $y\approx$ a few. There is, however, no obvious reason why observed α's in AGNs cluster tightly around the value 0.7.

4.2.2. Nonthermal Compton Scattering

(ii) and (iii) are essentially the same mechanism, the difference being that in the synchrotron-self-Compton (SSC) process the soft radiation to be upscattered is the synchrotron radiation produced by the scattering particles themselves. A spectral index of $\alpha=0.7$ requires a particle distribution $N(\gamma)$ with number index $p=2\alpha+1=2.4$. With cooling times being short this in turn requires a power law injection of particles $\dot{N}(\gamma)\propto\gamma^{-\Gamma}$ with $\Gamma=p+1=3.4$. The preference for $\alpha\approx0.7$ would have to be traced back to the not well understood acceleration and injection mechanisms. If electron-positron pairs are produced any $\Gamma<2$ may yield $\alpha\approx0.7$ (see §6).

4.3. Pair Production and Annihilation

Two additional processes are of uttermost importance in compact high energy plasmas: (1) photon-photon pair production in which two photons interact to produce an electron-positron pair, and (2) the reverse process, pair annihilation, in which an electron-positron pair selfdestruct to produce two photons.

It was early realized (e.g. [25],[26]) that a source could be optically thick to photon-photon pair production at a dimensionless photon energy ε (in units of mc^2) if the photon density, n_γ, at the photon energy $1/\varepsilon$ is large enough. The optical depth of a source of radius R with most photons at $\varepsilon\approx1$ is simply $\tau_{\gamma\gamma}\approx n_\gamma(\varepsilon\approx1)\sigma_T R\approx(L/4\pi R^2mc^3)\sigma_T R$, which is greater than unity for

$$\ell > 4\pi \approx 10 \qquad \text{or} \qquad \frac{L}{R} > 4\times10^{29}\ \text{erg s}^{-1}\text{cm}^{-1}. \tag{3}$$

More detailed considerations gives an energy and spectral shape depen-

https://doi.org/10.1017/S0252921100086152 Published online by Cambridge University Press

dent expression (see §6), but (3) shows the correct order of magnitude.

The pair annihilation process is of direct observational interest as it produces photons. Much work has been devoted to determining the thermal pair annihilation spectrum (e.g. [27]-[31]). The spectrum is most simply expressed as a single integral [30],[31]. At nonrelativistic temperatures the line is narrow, $\Delta\varepsilon/\varepsilon \approx (kT/mc^2)^{\frac{1}{2}}$, and centered on the rest mass energy 511 keV, while at relativistic temperatures the line mimics the annihilating particle distribution being broad ($\Delta\varepsilon/\varepsilon \approx 1$) and centered at the thermal energy kT. The pair annihilation cross section as well as the photon-photon pair production cross section suffer from the same Klein-Nishina decline at relativistic energies as the Compton scattering cross section. This causes the bremsstrahlung emission from annihilating pairs to dominate the annihilation emission as soon as kT is greater than a few mc^2, making the line invisible.

There are many marginally important processes not discussed here, but whose rates have recently been calculated [32]-[39]. We now turn to the effects of pair production in thermal and nonthermal plasmas considering dominant processes only.

5. Thermal Pair Production

The basic simplifying assumption in the study of thermal plasmas is that the particle distribution is thermal, i.e. the particles have a Maxwell-Boltzmann velocity distribution characterized by one single parameter alone, the temperature. Created particles (pairs) are assumed to instantaneously join the thermal distribution. This may not be the case in situations where e.g. the energy exchange time scale with a nonthermalized radiation field (which is what we observe) is much faster than the particle relaxation time scales.

Thermal pair equilibrium in static atmospheres has by far received most attention, while only a few studies have been done on time-dependent non-equilibrium pair atmospheres.

5.1. L/R-constraints in Thermal Pair Equilibrium

Thermal pair equilibrium (i.e. when pair production is balanced by pair annihilation and pair escape) has been considered in [35],[36],[40]-[49]. The discussion here partly follows that of [21]. Consider a uniform spherical plasma cloud in which the spectral density of photons with energy ε (in units of mc^2) is given by

$$n(\varepsilon) = \tfrac{1}{2} N_\gamma (\varepsilon/\theta)^{-\alpha} \exp(-\varepsilon/\theta)/\varepsilon, \qquad (4)$$

where α is the spectral index at low energies, N_γ is a normalization factor related to the total photon density, and θ is the cutoff energy of the spectrum. The photon density is approximately equal to the photon generation rate times the diffusive photon escape time $(1+\tau)R/c$. Then the compactness of the cloud is expressed as

$$\ell \approx 6 \frac{N_\gamma}{n_e} \theta \min(1,\tau), \qquad (5)$$

where n_e is the total density of electrons and positrons. (Coefficients when included are evaluated for $\alpha=0.7$). It remains to determine the ratio N_γ/n_e (and τ when $\tau<1$) as a function of the temperature θ and the slope α! N_γ/n_e is obtained from the pair equilibrium equation,

$$\left(\frac{N_\gamma}{n_e}\right)^2 f_{\gamma\gamma} + f_{ee} = f_A + \frac{\beta_{esc}}{\tau}, \qquad (6)$$

https://doi.org/10.1017/S0252921100086152 Published online by Cambridge University Press

where only the processes relevant for our discussion have been included. As the upper limit on ℓ (or N_γ/n_e) is to be determined, (6) is written for the case of a pair dominated plasma, where N_γ/n_e is maximized. The two terms on the left hand side represent the pair production rate due to $\gamma\gamma \to e^+e^-$ and $ee \to eee^+e^-$ while the two right hand side terms represent pair annihilation and a phenomenological escape term ($\beta_{esc} = v_{esc}/c$). The f-factors are temperature dependent rate coefficients [21]. Two separate cases may be considered, one where pair annihilation dominates and the other where pair escape dominates.

5.1.1. Pair Annihilation Dominates

In this case $N_\gamma/n_e = ((f_A - f_{ee})/f_{\gamma\gamma})^{\frac{1}{2}}$. As the annihilation rate decreases with temperature, while the rate coefficient f_{ee} increases, N_γ/n_e (as well as ℓ) goes to zero at some finite temperature determined by $f_A = f_{ee}$. Above this temperature, $\theta \approx 24$ or $T \approx 10^{11}$K, pair annihilations cannot keep up with particle-particle pair production and pair equilibrium is not possible [40].

At nonrelativistic temperatures, $\theta < 1$, and for τ large enough (at least >1) Comptonization causes a Wien tail to be established at pair producing energies $\varepsilon \approx 1$. The Comptonization can either be saturated ($\theta\tau^2 >> 1$) with a fully developed Wien peak or unsaturated ($\theta\tau^2 \approx 1$) with only the high energy tail of the photon distribution having a Wien shape. In either case the constraints from pair equilibrium considerations are the same. One should also note that for $\theta < 1$ and $\tau > 1$ pair annihilation always dominate pair escape (as $f_A \approx 1$ for $\theta < 1$). As $N_\gamma/n_e = (f_A/f_{\gamma\gamma})^{\frac{1}{2}} \approx \theta^{3/2}\exp(1/\theta)$ the maximum compactness becomes

$$\ell_{max} \approx 10\theta^{5/2}\exp(1/\theta), \tag{7}$$

as was first shown in [36] for the fully saturated case.

For $1 \lesssim \theta \lesssim 24$ it is necessary to specify the dominant radiation process. In the case of unsaturated relativistic Comptonization of soft photons a power law is produced with spectral slope $\alpha \approx \log(1/\tau)/\log(16\theta^2)$, which can be rewritten as $\tau \approx (4\theta)^{-2\alpha}$ (<1 for $\theta > 1$). As $N_\gamma/n_e = (f_A/f_{\gamma\gamma})^{\frac{1}{2}} \approx \theta^{-1-\alpha}$ the constraint on the compactness at a given α and for $1 \lesssim \theta \lesssim 24$ is

$$\ell_{max} \approx \theta^{-3\alpha}, \tag{8}$$

with a constant of order unity [21].

The dashed and solid curves in Fig.1 show the cases when Comptonized bremsstrahlung and unsaturated Comptonization of soft photons are dominant radiation mechanisms, respectively (from detailed calculations in [36], [21]). The two curves merge at $\theta << 1$, where (7) is valid and at $\theta \approx 24$.

5.1.2. Pair Escape Dominates

Pair escape can only dominate at $\theta > 1$ as discussed previously. For Comptonization of soft photons $N_\gamma/n_e = (\beta_{esc}/\tau f_{\gamma\gamma})^{\frac{1}{2}} \approx \beta_{esc}^{\frac{1}{2}}$ as $\tau \approx (4\theta)^{-2\alpha}$ and $f_{\gamma\gamma} \approx \theta^{2\alpha}$. The maximum value of ℓ becomes [21]

$$\ell_{max} \approx 10\beta_{esc}^{\frac{1}{2}}\,\theta^{1-2\alpha}. \tag{9}$$

The dotted curve in Fig.1 shows ℓ_{max} when $\beta_{esc} = 1$. Equation (9) describes the behavior of ℓ_{max} for $\theta > 1$. For $\theta << 1$ pair annihilation dominates and (6) is valid.

https://doi.org/10.1017/S0252921100086152 Published online by Cambridge University Press

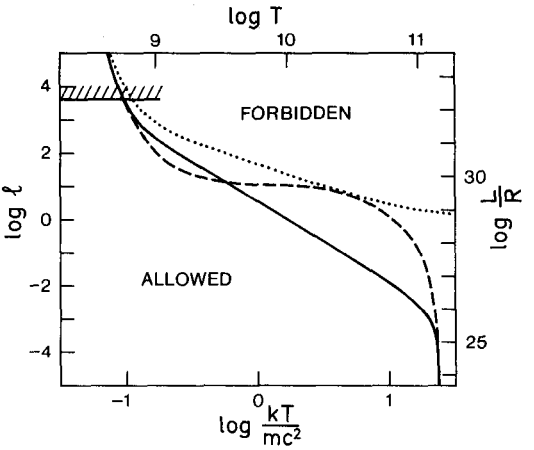

Fig.1. The maximum compactness $(L/R)_{max}=4\times10^{28}\ell_{max}$ erg $s^{-1}cm^{-1}$ as a function of the temperature T. The region above the curves are forbidden for spherical clouds in thermal pair equilibrium. The dominant radiation processis Comptonized bremsstrahlung for the dashed curve and Comptonized soft photons with slope $\alpha=0.7$ for the other two curves. The dominant pair destruction mechanism is pair escape for the dotted curve and pair annihilation for the other two. The pair-free Eddington limit is violated for $\ell>4000$.

5.2. Further Aspects of Thermal Pair Production

5.2.1. Two Pair Branches

Besides the pair dominated equilibrium cloud there also exists the possibility of having a cloud in pair equilibrium with the pair density being much smaller than the density of the electrons associated with the protons of the plasma. The small fraction of pairs present does not affect the cloud luminosity. In the case of bremsstrahlung at $\theta>1$ the compactness becomes

$$\ell \approx 0.1\tau_p^2\theta\ln\theta, \qquad (10)$$

where τ_p is the Thomson scattering depth of the ionization electrons. The curves in Fig.2 show the behavior of ℓ at a given τ_p in the case when no prolific source of soft photons is present. At some temperature the low-pair curves join the envelope formed by the pair dominated curve, ℓ_{max}, discussed in the previous section. As the compactness of a source increases, the temperature first increases (e.g.(10)) until the plasma becomes pair dominated. Increasing ℓ further causes the temperature to decrease (see (7)-(9)).

5.2.2. The Pair Annihilation Line

A pair annihilation line is in general not seen from a uniform cloud in pair equilibrium. At relativistic temperatures other emission processes dominate (see §4.3), and at nonrelativistic temperatures the optical depths to Compton scattering and photon-photon pair production are large enough to modify the annihilation line into a Wien tail (in pair dominated plasmas) [21],[36].

https://doi.org/10.1017/S0252921100086152 Published online by Cambridge University Press

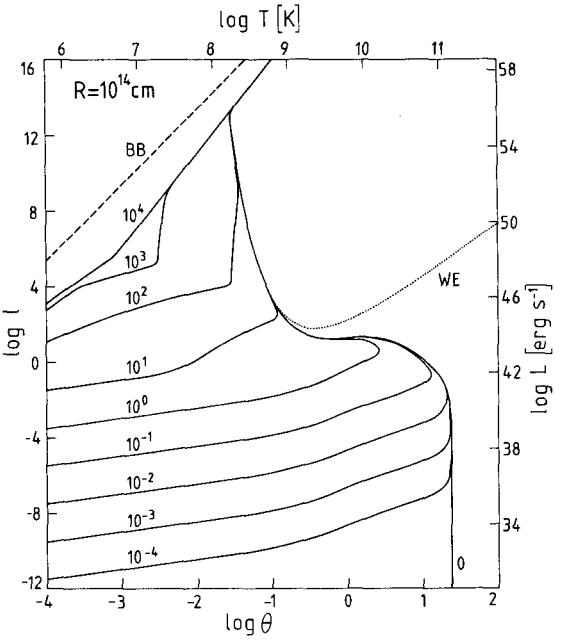

Fig.2. The compactness $L/R=4\times10^{28}\ell$ erg $s^{-1}cm^{-1}$ as a function of the temperature $\theta=kT/m_ec^2$ for a spherical magnetic field-free cloud in thermal pair equilibrium. The Thomson depth, τ_p, of the ionization electrons label each solid curve. The dotted curve shows ℓ for a pair dominated cloud in Wien equilibrium (see (6)). The region above the envelope curve is forbidden for pair equilibrium clouds. From [30].

5.2.3. Thermal Pair Production in Accretion Flows

Pair equilibrium in the accretion flow of hot geometrically thick two-temperature tori is possible when the following three conditions are satisfied [3],[50]: (1) the annihilation time scale should be less than the inflow time scale for pair equilibrium to be established, (2) the pair density should exceed the ion density for pairs to be important, and (3) the pairs and the ions should stay decoupled to keep the ions hot. These conditions outline a region in the viscosity-accretion rate parameter space where pair equilibrium can be established (moderate to high viscosities and slightly subEddington accretion rates). The detailed structure of these disks with or without pairs is not known and awaits a better understanding of the dissipation mechanisms. In the meantime simple uniform cloud models will do. Adding phenomenological accretion terms to the time dependent density and energy equations [47] it was found [51] that the system showed limit cycle behavior with high energy flares near $\ell\approx10$. The pairs were assumed to be heated in Coulomb collisions with the protons and to cool by Comptonized bremsstrahlung.

6. Nonthermal Pair Production

The particle distribution in nonthermal models is often solved for self-consistently given several assumptions regarding the acceleration and/or injection processes. Normally a particle injection spectrum is prescribed (requiring several parameters) whereupon the steady cooled particle

https://doi.org/10.1017/S0252921100086152 Published online by Cambridge University Press

spectrum can be determined given the cooling processes (requiring the specification of additional parameters). The observations of X-ray(power law) spectra provides only few observables (slope, flux, variability time scales) and do not discriminate very well among competing nonthermal models. Future observations in the hard X-ray and γ-ray range may, however, show breaks and bends as well as an annihilation line related to nonthermal pair production improving the ratio of the number of observables to the number of theoretical parameters.

It was already realized by BONOMETTO and REES in 1971 [52]that nonthermal pair production causes a redistribution (or reprocessing) through pair cascades of injected particle energy from high energies towards smaller energies making the secondary (pair and photon) injection to approach a state where equal power is injected per logarithmic energy interval. The observed photon spectrum is however, not necessarily equal to the injected photon spectrum, but is affected by various opacity effects introducing spectral breaks.

Although the same basic radiation mechanisms are employed, published models [17],[24],[52]-[59] differ in the following respects:

(i) The choice of whether the Compton scattering takes place on external soft photons narrowly distributed in energy or on the internal broad band radiation produced by the scattering particles themselves. In the former case the energy of the injected particles can be chosen such that the scattering in the cascade is in the Thomson limit [55]-[58], or in the Klein-Nishina limit [59]. Compton scatterings on internally generated radiation take place in both limits often with the dominant scatterings occurring in the Thomson- Klein-Nishina boundary [52],[54]. In sources where a Planck spectrum (from a cool accretion disk) near a photon energy $\varepsilon_s \approx 10^{-5}$ is the dominant soft photon source, the cascades are mostly of the Thomson type as $\gamma_{drag}\varepsilon_s \approx 1$. The appealing features of a Thomson cascade in an external soft photon medium is the lack of nonlinearity and the small number of generations making an analytical treatment possible.

(ii) The choice of whether the particle injection is isotropic and uniform in an extended region [17],[24],[52],[53],[55]-[58] or whether the injection is anisotropic in some respect [54],[59]. In the former case later cascade generations interact with generations of all ages, while in the latter case it may be that interactions only take place between particles and photons of equal ages (cascade shower).

(iii) The choice of whether the particles are injected monoenergetically or as a power law with suitable cutoffs.

Most analytical results(to be summarized below)have been obtained for the case of Thomson cascades on external soft photons taking place in a region having uniform particle injection of the monoenergetic type.

6.1. Thomson Cascades with Monoenergetic Injection

Consider a spherical region of size R, where a luminosity L is injected uniformly as relativistic monoenergetic particles with a Lorentz factor $\gamma_{max} >> 1$. The injected particles cool by inverse Compton scatterings in the Thomson limit on externally generated photons at the photon energy $\varepsilon_s << 1$. As most of the particle luminosity is converted into radiation, selfconsistency requires the energy density of external photons at ε_s to exceed the energy density of the photons emitted by the cooling particles. When the injected particles cool (with the cooling $\dot{\gamma} \propto \gamma^2$), the resulting particle distribution is $N(\gamma) \propto 1/\dot{\gamma} \propto \gamma^{-p}$ with p=2 and the Compton scattered photons, extending from ε_s to $\varepsilon_{max} \approx \gamma_{max}^2 \varepsilon_s$, have a spectral

https://doi.org/10.1017/S0252921100086152 Published online by Cambridge University Press

index $\alpha=(p-1)/2=0.5$ and an integrated luminosity L.

A photon of energy $\varepsilon>>1$ interacts with a photon of energy $1/\varepsilon$ to produce an electron-positron pair, each particle having an energy $\varepsilon/2$. The injected pairs Thomson cool, just as the primary particles, giving rise to more Compton scattered photons. If these extend beyond mc^2, then a second pair generation is injected that Compton scatters further photons. This pair cascade continues until the last Compton scattered photon generation has a too small maximum photon energy to make further pairs. Using a simple treatment of the radiation transfer ZDZIARSKI and LIGHTMAN [57] showed that the steady photon and pair distributions including all generations are determined by a rather simple integral equation. Analytical solutions of this equation in the low [57] and high [58] luminosity limit reveal many of the properties of nonthermal pair production. Numerical solutions in a different formulation [55] show similar properties.

6.2. The Pair Yield

A convenient parameter to describe the amount of created pairs is the pair yield, x, i.e. the fraction of injected luninosity that is converted into pair rest mass. The Thomson scattering optical depth of pairs is simply related to the pair yield (using the balance between the creation and annihilation of pairs) [17]

$$\tau = (x\ell/g)^{\frac{1}{2}}, \tag{11}$$

where $g>1$ is a low temperature correction factor to the Born annihilation rate describing Coulomb effects and positronium formation.

Figure 3 shows the pair yield as a function of injection luminosity for two cases, one where there is three generations of pairs (solid curve), and one where there is only one (dashed curve). There are three characteristic regions: 1) a low luminosity region with few pairs, 2) a transition region near the critical luminosity, ℓ_c, where the plasma changes from an essentially pair free state to a pair dominated state, and 3) a high luminosity region where pair production is saturated, i.e. the pair yield has reached its maximum value (close to unity).

The optical depth to photon-photon absorption at the photon energy ε in a radiation field with spectral index α in a source of compactness ℓ is given by

$$\tau_{\gamma\gamma}(\varepsilon) \approx 0.2\sigma_T Rn(1/\varepsilon)/\varepsilon \approx (\ell/40)(\varepsilon\varepsilon_{max})^{\alpha}/\varepsilon_{max}, \tag{12}$$

where the coefficient was evaluated for $\alpha=0.5$. $\tau_{\gamma\gamma}$ is much less than unity for all $\varepsilon<\varepsilon_{max}$ when $\ell<<40$. In such a transparent source there is very little pair production with the pair yield increasing linearly with ℓ [58]

$$x \approx 0.01\ell \frac{\ln \varepsilon_{max}}{\varepsilon_{max}} << 1. \tag{13}$$

Even a small redistribution (by the pair cascade) of the radiation at ε_{max} (where most of the spectral energy density is) towards smaller energies will have a large effect on the small energy density at the photon energy $1/\varepsilon_{max}$ and hence on $\tau_{\gamma\gamma}(\varepsilon_{max})$. Increasing $\tau_{\gamma\gamma}(\varepsilon_{max})$ redistributes even more energy towards $1/\varepsilon_{max}$ and there is a nonlinear runaway production of pairs at a luminosity, ℓ_c, much smaller than 40, as shown in Fig.3. The pair yield increases with up to several orders of magnitude at ℓ_c until it saturates at $x\approx 10\%$.

https://doi.org/10.1017/S0252921100086152 Published online by Cambridge University Press

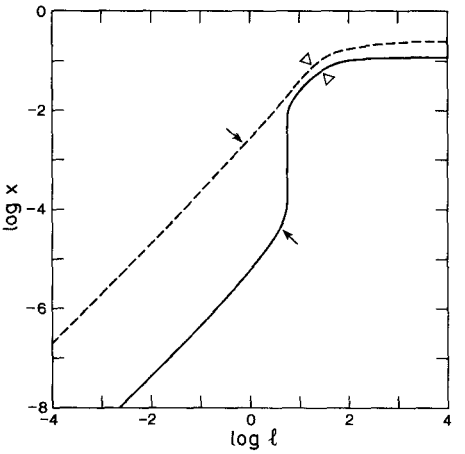

Fig.3. The pair yield, x, as a function of the dimensionless injection luminosity (or compactness), ℓ, for the case of monoenergetic injection of particles with Lorentz factor $\gamma_{max}\approx 470$ (dashed curve) and 2.7×10^4 (solid curve). The particles Thomson-cool on soft photons injected at $\varepsilon_s=2.7\times10^{-5}$. The maximum photon energy is then $\varepsilon_{max}=8$ and 2.6×10^4 for respective case. Above the arrows the produced pairs dominate (by number) the injected particles. The triangles show where the Thomson scattering optical depth of cool pairs becomes unity. From [58].

The saturation magnitude is an easily determined function of ε_s and ε_{max} [58]. The maximum pair yield occurs when there is only one pair generation. Then

$$x = \left(\frac{2}{\varepsilon_{max}}\right)^{\frac{1}{2}} - \frac{2}{\varepsilon_{max}} \qquad (\ \ell >> \ell_c\ ) \qquad (14)$$

which has the peak value x=1/4 =25% at $\varepsilon_{max}=8$ (dashed curve in Fig.3). The Thomson depth of the cool pairs in saturated nonthermal pair plasmas becomes as large as $\tau\approx 20(\ell/4000g)^{\frac{1}{2}}$. These cool pairs reprocess both the nonthermal continuum radiation and any external soft radiation.

6.3. The Pair Cascade

When the pair cascade is important (i.e. when $\ell>\ell_c$) and the pair density exceeds the density of injected particles, then the injected energy distribution is no longer $\varepsilon\dot{n}(\varepsilon)\propto\varepsilon^{-\alpha}$ with $\alpha=\frac{1}{2}$ but it is the sum over all photon generations in the cascade. For saturated ($\tau_{\gamma\gamma}>>1$) nonthermal pair production the different photon generations can be solved for analytically [58]. Figure 4 shows both the injected photon generations as well as their sum . The following conclusions are made:

1) For $\ell<<\ell_c$ the photon energy injection has the spectral index $\alpha=\frac{1}{2}$ with most of the power being injected near ε_{max}.

2) For $\ell>>\ell_c$ the pair cascade causes a redistribution of the photon energy injection towards almost equal power per logarithmic energy interval, i.e. $\alpha=1$ or $\varepsilon^2\dot{n}(\varepsilon)$ constant.

3) The injected photon distribution is in general <u>not</u> a power law although devations are small for $\ell>>\ell_c$ and for $\ell<<\ell_c$.

The redistribution from $\alpha=\frac{1}{2}$ towards $\alpha=1$ comes about as follows. The photons from the injected particles have $\alpha_0=\frac{1}{2}$. In the saturated case they all produce pairs making the pair injection $P(\gamma)\propto\gamma^{-1}$ to have $\Gamma_1=\alpha_0+1=3/2$. Cooling causes the first pair generation to have $N(\gamma)\propto\gamma^{-p_1}$

https://doi.org/10.1017/S0252921100086152 Published online by Cambridge University Press

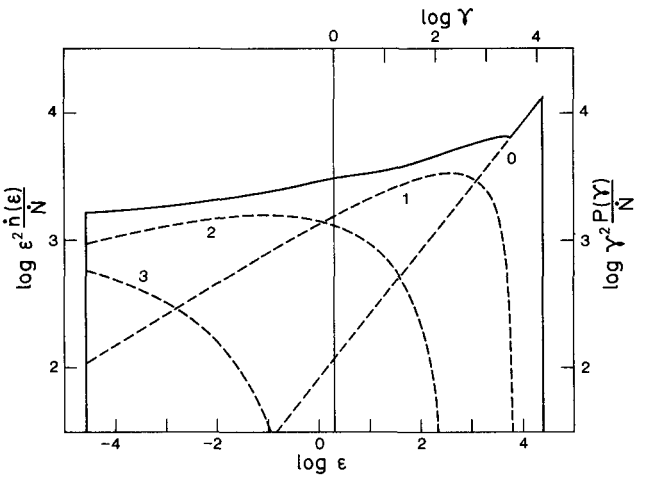

Fig.4. The injected photon ($\dot{n}(\varepsilon)\,cm^{-3}s^{-1}$) and pair ($P(\gamma)\ cm^{-3}s^{-1}$) spectra (shown as dimensionless injected power per logarithmic energy interval, $\dot{N}$ is the injection rate of primary particles) as functions of the photon energy ε (in units of mc^2) and Lorentz factor γ in the fully saturated case. All injected photons above threshold make pairs causing the distributions to be identical $P(\gamma)=\dot{n}(\varepsilon=2\gamma)4$. The dashed curves show the photon injection by the primary particles (labelled 0) and by the three pair generations (labelled 1-3). The sum of the different generations is shown by the solid curve. Primary particles are injected at $\gamma_{max}=2.7\times10^4$ and soft photons at $\varepsilon_s=2.7\times10^{-5}$. From [58].

with $p_1=\Gamma_1+1=5/2$. Then the spectral index of the first photon generation caused by pairs is $\alpha_1=(p_1-1)/2=0.75$. Continuing the argument gives for the i^{th} generation $\Gamma_i=2-1/2^i$, $p_i=3-1/2^i$, and $\alpha_i=1-1/2^{i+1}$ with $\alpha_2=0.875$ and $\alpha_3=0.9375$. As Thomson cascades have at most a few generations, α_i never becomes unity (the equilibrium argument in [56] giving $\alpha=1$ requires a large number of generations). Figure 4 shows that only the low energy part of each generation has the index α_i. Different photon generations dominate the injected photon distribution at different energies. The injected power per logarithmic energy interval in the saturated case is nevertheless approximately constant as almost all photon energy in a given generation (except for the part below threshold $\varepsilon\approx2$) gets reprocessed into the next generation. The loss below threshold is partly compensated for by the smaller energy range of the next generation. The X-ray region is normally dominated by one of the last two generations.

Figure 5 shows how the emerging photon power per logarithmic energy interval at the surface of the pair cloud changes due to spectral reprocessing as ℓ increases from small values to its maximum possible value of about 4000. For small ℓ the emerging spectrum is simply the radiation (with $\alpha=\frac{1}{2}$) from the cooling primary particles. As ℓ increases past ℓ_c (from 4 to 6 in Fig.5) the spectrum changes drastically due to the effects of the pair cascade. Most of the injected γ-ray energy gets reprocessed into the X-ray range and the X-ray luminosity increases by several orders of magnitude.

The emerging radiation above the photon energy ε_{abs} at which $\tau_{\gamma\gamma}(\varepsilon_{abs})=1$ is affected by photon absorption in photon-photon collisions. The optically thick emission emerges from a narrow surface layer of thickness $R/\tau_{\gamma\gamma}(\varepsilon)$ and the spectral luminosity steepens from $d\ell/d\varepsilon\propto\varepsilon\dot{n}(\varepsilon)\propto\varepsilon^{-\alpha}$

https://doi.org/10.1017/S0252921100086152 Published online by Cambridge University Press

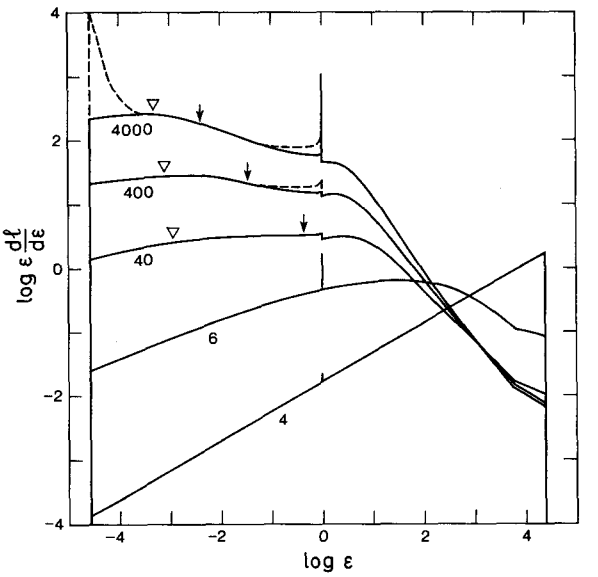

Fig.5. The photon spectrum (shown as the dimensionless spectral luminosity per logarithmic energy interval) as a function of the photon energy ε (in units of mc^2). Curves are labeled with the compactness ℓ. A particle luminosity ℓ is injected at $\gamma_{max}=2.7\times10^4$ and a dominant soft photon luminosity is injected at $\varepsilon_s=2.7\times10^{-5}$. There is a strong redistribution of the injected luminosity at γ_{max} towards ε_s as various redistribution processes (pair cascades, downscatterings) becomes effective with increasing compactness ℓ. The triangles show the decreasing pair temperatures with increasing ℓ, while the arrows show the break frequency, $\varepsilon_{break}=1/\tau^2$, due to downscatterings. Dashed curves show the contributions of upscattered soft photons and downscattered annihilation photons. The surface cascade, not taken into account, would cause further degrading at $\varepsilon\gtrsim1$. From [58].

below ε_{abs} to approximately $d\ell/d\varepsilon\propto\varepsilon\dot{n}(\varepsilon)/\tau_{\gamma\gamma}(\varepsilon)\propto\varepsilon^{-2\alpha}$ above ε_{abs} with $\alpha\lesssim1$ as is shown by the high luminosity curves in Fig.5. If no other opacity effects are present then for saturated pair plasmas ε_{abs} is of order unity withalmost all luminosity emerging below ε_{abs}. The only numerical study so far of radiative transfer with pair absorption (neglecting, however, all other reprocessing) [60] have low energy resolution but show the expected absorption behavior.

6.4. Thermal Compton Scatterings

The injected luminosity is not only reprocessed by the relativistic pair cascade but also by the cooled nonrelativistic thermal pairs whenever τ is larger than unity. This is normally the case when the pair plasma is saturated. The temperature of the pairs is determined by Compton cooling on the soft external photons (of luminosity $L_{soft}>>L$) and by Compton heating on the scattered radiation field of luminosity L extending from ε_s up to $\varepsilon_{abs}\approx1$. The cooling rate is approximately yL_{soft}, where y is the Compton parameter $4\tau^2kT/mc^2$ and the heating rate is fL with f<1(as most photons between $\varepsilon_{break}=1/\tau^2\approx1/(x\ell)$ and ε_{abs} gets downscattered to ε_{break}). The steady pair temperature is then

https://doi.org/10.1017/S0252921100086152 Published online by Cambridge University Press

$$kT_{pair} \approx 0.25mc^2 \, f/(x\ell_{soft}) << 1 \, . \qquad (15)$$

The curve for ℓ=4000 in Fig.5 shows the result of taking all opacity effects into account:

1) There is a steep component of soft radiation upscattered by the cool pairs.

2) Below ε_{break} the continuum spectral shape is that of the nonthermal cascade photons, $\alpha \lesssim 1$.

3) Above ε_{break} downscattering on cool pairs steepens the spectral index from α to $\alpha+\frac{1}{2}$ [18].

4) The decrease in intensity between ε_{break} and $\varepsilon_{abs} \approx 1$ decreases $\tau_{\gamma\gamma}$ between ε=1 and $1/\varepsilon_{break}$ causing less photon absorption.

Finally there is the contribution from scattered and unscattered annihilation photons.

6.5. The Pair Annihilation Photons

The ratio of the annihilation luminosity, L_A, to the continuum luminosity L is simply equal to the pair yield x for τ<1, while there is a reduction by a factor $\tau \approx (x\ell)^{-\frac{1}{2}}$ for τ>1 making $L_A/L=(x/\ell)^{\frac{1}{2}}$. Thus, L_A/L has a maximum value of about 10% when $\tau \approx 1$. The narrow line is shown in a few cases in Fig.5. The line is however easily broadened into invisibility by random motions in the cloud or by thermal motions if the pairs are hotter than expected from the Compton heating/cooling balance.

There are some further annihilation contributions of marginal importance:

1) It is easily shown that annihilation photons from cool pairs rather downscatter than pair-produce. When τ>1 the downscattered fraction of the annihilation photons are distributed between ε_{break} and ε=1. The emerging spectral shape depends on the spatial distribution of pairs (a uniform distribution gives α=-0.5 [18]).

2) When $kT_{pair} << mc^2$ then three-photon-annihilation through positronium formation occurs [61], emitting a continuum ranging up to ε=1 with α=-1 [62]. A fraction $1/\tau$ emerges unscattered and the rest downscatters towards ε_{break} before escaping.

6.6. The Surface Cascade

It has not been sufficiently recognized that γ-ray photons above pair production threshold when leaving the pair photosphere of the uniform injection region enters a photon atmosphere that has a photon photosphere (due to photon-photon absorptions) at a radius much larger than the pair photosphere (when $\ell >> \ell_c$). The photon atmosphere mainly consists of the X-ray photons emerging from the pair photosphere. This radiation field becomes increasingly anisotropic at larger distances from the pair photosphere and the location of the photon photosphere (defined by $\tau_{\gamma\gamma}$=1) is energy and angle dependent. γ-rays photons initiate cascade showers as they leave the pair photosphere. The question is whether or not the showers are able to break out of the photon photosphere before being completely degraded to energies of the order mc^2. Thomson cascades probably do not (due to their small number of generations) and all the γ-ray energy injected into the photon photosphere probably emerges near $\varepsilon \approx mc^2$ with an exponential cutoff at larger energies. This last cascade does not change the emerging X-ray spectrum into which most of the injected energy already has been reprocessed (for $\ell > \ell_c$).

https://doi.org/10.1017/S0252921100086152 Published online by Cambridge University Press

6.7. Universal Spectral Slopes in AGNs

Spectral reprocessing by nonthermal pair production has been used to explain various slopes in the continuum spectra of AGNs. That the particle distribution index approaches 3 at large compactnesses was used in [56] to explain the $\alpha=1$ behavior from the IR to the UV in many objects. It was argued in [57] that the universal X-ray slope of $\alpha=0.7$ in most AGNs (having values of L_X/R covering two or three orders of magnitude) was due to spectral reprocessing by pairs. As shown in Fig.5 the X-ray slope changes from 0.5 to 0.9 while L_X/R varies by several orders of magnitude. We note, however, that the injection compactness, L/R, varies over a very narrow range as the slope changes from 0.5 to 0.9. Sources with varying injection compactness ℓ (or L/R) are expected mostly to be found either in the pair-free state with $\ell<\ell_c$ and $\alpha_X=0.5$ or in the pair saturated state with $\ell>\ell_c$ and $\alpha_X\approx 1$ (with possible further steepening due to downscatter or up scattered soft components). A bimodal distributionof spectral slopes is expected unless some mechanism locks the compactness at precisely ℓ_c.

6.8. Nonthermal Pair Production in Other Models

The effects of changing some of the assumptions in the model discussed so far (§6.1-§6.7) are slight or predictable.

Power law injection of particles with $\Gamma<2$ gives similar results as for monoenergetic injection. When $\Gamma>2$ most of the power radiated by the primary particles is already at small photon energies ($\alpha>1$) making reprocessing by pairs unimportant [24],[56],[57].

Cooling on internal radiation also causes the reprocessed injection to have equal power per logarithmic energy interval [52]. The detailed reason for this is not known (most likely being similar to those discussed in §6.3). An important difference as compared with the external soft photon case is that there is no characteristic energy, ε_s, set by the external radiation field and towards which partial 'thermalization' of pairs and photons can occur. Instead the characteristic energy will be the rest mass energy of the electron, $m_e c^2$. Redistributing processes will cause the pair temperature and the reprocessed radiation temperature to be of the order of $m_e c^2$.

Monte Carlo simulations of cascade showers [54] show that the pair yield reaches maximum levels of 10% or so, similar to the saturated pair yields of §6.2.

7. The Radiation-hydrodynamics of Pair Plasmas

A detailed understanding of the radiation hydrodynamics of pair plasmas (which really should have been the topic of this review) is presently lacking as the tools for treating radiative transfer of continuum and annihilation line radiation in mildly relativistic, marginally optically thick flows are not available. Some qualitative considerations can, however, be made.

Thermal plasmas in pair equilibrium at mildly relativistic temperatures as well as nonthermal plasmas become pair dominated when $\ell \gtrsim$ a few, or, equivalently,

$$L > \left(\frac{m_e}{m_p}\right) L_E \left(\frac{R}{3R_s}\right). \qquad (16)$$

Radiation pressure on pairs wins over gravity when

https://doi.org/10.1017/S0252921100086152 Published online by Cambridge University Press

$$L > L_{E,pair} = \left(\frac{m_e}{m_p}\right) L_E. \qquad (17)$$

Thus, when pairs are produced and $R>3R_s$ then the source is super-Eddington and the pairs will expand as a radiatively driven wind. In nonthermal pair atmospheres the radiation is generally trapped as the Thomson depth of cool pairs $\tau\approx(x\ell)^{\frac{1}{2}}$ is greater than unity (for $\ell>\ell_c$) and the ratio of radiation energy density to pair rest mass energy density is $(\ell/x)^{\frac{1}{2}}>1$, necessitating relativistic flows. Similar conditions hold in pair dominated thermal pair atmospheres.

A pair atmosphere expanding into a wind is characterized by three regions [3],[47]: 1) the energy injection region, 2) the adiabatic expansion and annihilation region, and 3) the radiatively driven wind region.

1) Pair equilibrium holds in most of the energy injection region. Here, the flow is subsonic and the flow time, $>R/c$, exceeds the pair creation time. The pair density rapidly adjusts to a level where pair annihilations balances pair creations. The conditions in this region strongly resembles those of the static clouds discussed above in §5,§6.

2) Outside the radius, R, where the energy injection ceases, radiation and gas convect together supersonically with a bulk Lorentz factor $\gamma\approx 1.2r/R$. This adiabatic expansion ceases at the trapping radius, R_{trap}, where the comoving scattering depth drops to unity and where the radiation decouples from the gas. The comoving scattering optical depth depends on the pair density, that rapidly drops throughout this region as pair annihilation is no longer balanced by pair creations. With decreasing pair density the annihilation time scale eventually becomes larger than the flow time, defining the pair freeze-out-radius, R_A. A simple analysis [3],[47] gives $R_A\approx R_{trap}\approx 1.5R$ with $\gamma(R_A)\approx 2$. The luminosity in pair rest mass, L_{pair}, carried across R_A (or R_{trap}) is $L_{pair}\approx 2n_{pair}(R_A)mc^2c4\pi R_A^2\approx(mc^3/\sigma_T)R$ as $\tau(R_A)\approx$ a few and neglecting some mildly relativistic correction factors. Thus $\ell_{pair}\approx$ unity, which is independent of the injected luminosity ℓ. Even if 10% of $\ell>>1$ is converted into rest mass only $\ell_{pair}\approx 1$ emerges as pair rest mass luminosity due to the annihilations between R and R_A.

3) In the radiatively driven wind region outside R_A radiation pressure accelerates the pairs to even larger Lorentz factors. Eventually a Lorentz factor is reached where, in the rest frame of the outflowing pairs, the extended radiation source of size R_A will appear to cover the backward hemisphere and to start filling the forward hemisphere. The photons aberrated into the forward direction will cause Compton drag, limiting the final Lorentz factor of the flow to $\gamma\approx \ell^{1/4} \lesssim 8$ as ℓ is smaller than 4000 [63],[64]. The rest mass and kinetic luminosity of the wind never exceed some 10% of the injected luminosity, a fraction decreasing with increasing compactness for $\ell>>1$ [3].

8. Final Thoughts

Processes in physical systems normally act to bring the system towards some state of equilibrium. In particular, nonequilibrium particles and photons in astrophysical systems interact to come into equilibrium with each other. In finite systems, however, the residence time of photons and/or particles is often too small for complete thermalization to be achieved. We have reviewed recent studies of two such physical systems, where the particles and photons have energies larger than m_ec^2 allowing both photons and pairs to be produced.

https://doi.org/10.1017/S0252921100086152 Published online by Cambridge University Press

Firstly, we considered a system, where all particles and pairs are thermal at some specified temperature and where the produced radiation tries to reach equilibrium with the particles before escaping the system. Produced pairs annihilate at the prescribed temperature and it was found that steady state (thermal pair equilibrium) was not possible for certain combinations of temperature and compactness.

Secondly, we considered a nonthermal system, where luminosity was injected at energies $>>m_e c^2$ and at energies $<<m_e c^2$ (the injection at energies $>>m_e c^2$ was assumed to be particles but could just as well have been photons). If the optical depths of the system are large enough (>1) then interactions take place to bring the hard radiation field into equilibrium with the (dominant) soft radiation field. Increasing the compactness brings additional thermalizing effects into action (Fig.5). Even at the largest allowed compactness (consistent with gravitational energy release) the thermalization is far from complete.

Only in the highly luminous conditions near collapsed objects such as neutron stars and black holes will we ever be able to observe the result of the three processes of the lowest order Feynman diagram operating in unison. The opacity effects of two of them (Compton scattering below $m_e c^2$ and photon-photon absorption above $m_e c^2$) straddles the emission from the third (pair annihilation at $m_e c^2$). Hopefully these three processes around $m_e c^2$ will eventually help us to increase our knowledge of the conditions in and the spatial structure of luminous compact objects. However, if we are to learn from what opacity effects at the other end of the spectrum (synchrotron self absorption) brought us in terms of diagnostic value, we should not put our hopes too high.

Acknowledgements

Thanks are due to Andrzej Zdziarski and Alan Lightman for writing a stimulating paper.

References

1. Begelman,M.C.,Blandford,R.D.,and Rees,M.J.:Rev.Mod.Phys.,56,255(1984).
2. Rees,M.J.,Ann.Rev.Astr.Ap.:22,471(1984).
3. Phinney,E.S.:Ph.D.thesis,University of Cambridge(1983).
4. Svensson,R.:in X-ray and UV Emission from Active Galactic Nuclei edited by J.Trümper and W.Brinkman(Max-Planck,Garching,1984)p.152.
5. R.Petre,R.F.Mushotzky,J.H.Krolik,and Holt,S.S. :Astroph.J.,280,499 (1984).
6. Rothschild,R.E.et al.:Astroph.J.,269,423(1983).
7. Elvis,M.,Wilkes,B.J.,and Tananbaum,H.:Astroph.J.,292,357.
8. Elvis,M,:Center for Astroph. Preprint No.2126 (1985).
9. Perotti,F. et al.:Nature,292,133(1981).
10. Perotti,F.et al.:Astroph.J.Lett.,247,L63(1981).
11. Bezler,M. et al.:Astron.Astr.,136,351(1984).
12. Tennant,A.F.,and Mushotzky,R.F.:Astroph.J.,264,92(1983).
13. Zamorani,G.,Giommi,P.,Maccacaro,T.,and Tananbaum,H.:Astroph.J.,278, 28(1984).
14. Bassani,L,and Dean,A.J.:Nature,294,332(1981).
15. Rybicki,G.B.,and Lightman,A.P.:Radiative Processes in Astrophysics (Wiley.Interscience,New York,1979).
16. Dermer,C.D.:preprint (1985).
17. Guilbert,P.W.,Fabian,A.C.,and Rees,M.J.:M.N.R.A.S.,205,593(1983).
18. Sunyaev,R.A.,and Titarchuk,L.G.:Astron.Astr.,86,121(1980).
19. Fransson,C.:AStron.Astr.,111,140(1982).

20. Pozdnyakov,L.A.,Sobol',I.M.,and Sunyaev,R.A.:Soviet Scientific Review,Section E2,(Harwood,London,1983),p.189.
21. Zdziarski,A.A.:Astroph.J.,289,514(1985).
22. Gőrecki,A.,and Wilczewski,W.:Acta Astr.,34,141(1984).
23. Guilbert,P.W.:M.N.R.A.S.,197,451(1981).
24. Zdziarski,A.A.:Astroph.J.,in press(1986).
25. Jelley,J.V.:Nature,211,472(1966).
26. Herterich,K.:Nature,250,311(1974).
27. Zdziarski,A.A.:Acta Astr.,30,371(1980).
28. Ramaty,R.,and Mészaros,P.:Astroph.J.250,384(1981).
29. Svensson,R.:Astroph.J.,258,321(1982).
30. Svensson,R.:Astroph.J.,270,300(1983).
31. Dermer,C.D.:Astroph.J.,280,328(1984).
32. Weaver,T.A.:Phys.Rev.,A13,1563(1976).
33. Lightman,A.P.,and Band,D.L.:Astroph.J.,251,713(1981).
34. Gould,R.J.:Astroph.J.,254,755(1982).
35. Svensson,R.:Astroph.J.,258,335(1982).
36. Svensson,R.:M.R.A.S.,209,175(1984).
37. Stepney,S.,and Guilbert,P.W.:M.N.R.A.S.,204,1269(1983).
38. Stepney,S.:M.N.R.A.S.,202,467(1983).
39. Dermer,C.D.:Astroph.J.,295,28(1985).
40. Bisnovatyi-Kogan,G.S.,Zeldovich,Ya.B.,and Sunyaev,R.A.:Sov.Astr., 15,17(1971).
41. Lightman,A.P.:Astroph.J.,253,842(1982).
42. Araki,S.,and Lightman,A.P.:Astroph.J.,269,49(1983).
43. Kusunose,M.,and Takahara,F.:Progr.Theor.Phys.,69,1443(1983).
44. Kusunose,M.,and Takahara,F.:Progr.Theor.Phys.,73,41(1985).
45. Zdziarski,A.A.:Astroph.J.,283,842(1984).
46. Zdziarski,A.A.:Astroph.J.,in press(1986).
47. Guilbert,P.W.,and Stepney,S.:M.R.A.S.,212,523(1985).
48. Schultz,A.L.,and Price,R.H.:Astroph.J.,291,1(1985).
49. Sikora,M.,and Zbyszewska,M.:M.N.R.A.S.,212,553(1985).
50. Takahara,F.,and Kusunose,M.:Progr.Theor.Phys.,73,1390(1985).
51. Moskalik,P.,and Sikora,M,:preprint(1985).
52. Bonometto,S.,and Rees,M.J.:M.N.R.A.S.,152,21(1971).
53. Aharonian,F.a.,Kirillov-Ugryumov,V.G.,and Vardanian,V.V.:preprint (1983).
54. Stern,B.E.:preprint(1984).
55. Fabian,A.C.:in X-ray and UV Emission from Active Galactic Nuclei edited by J. Trümper and W.Brinkman(MaxPlanck,Garching,1984)p.232.
56. Kazanas,D.:Astroph.J.,287,112(1984).
57. Zdziarski,A.A.,and Lightman,A.P.:Astroph.J.Lett.,294,L79(1985).
58. Svensson,R.:preprint(1985).
59. Burns,M.L.,and Lovelace,R.V.E.:Astroph.J.,262,87(1982).
60. Carrigan,B.J.,and Katz,J.I.:preprint(1985).
61. Crannell,C.J.,Joyce,G.,Ramaty,R.,and Werntz,C.:Astroph.J.,210,582 (1976).
62. Ore,A.,and Powell,J.L.:Phys.Rev.,75,1696(1949).
63. Noerdlinger,P.D.:Astroph.J.,192,529(1974).
64. Kovner,I.:Astr.Astroph.,141,341(1984)

Questions

Epstein: What is the expected spectrum of the γ-radiation from a pair wind?
Svensson: This is not yet known but the spectrum is probably similar to the high-compactness spectra in Fig.5 with some blue-shifts expected.
Epstein: Would asymmetric outflows give enough polarization to explain BL Lac observations?
Svensson: No, this would require extremely contrived geometries and line-of-sight directions.
Michel: Are ions important here? Naively one might expect them to load down these winds somewhat.
Svensson: Yes, n_{pair}/n_{ion} probably much reach a level of m_p/m_e for down-loading not to be important. Photon-photon interactions may however create pairs in essentially ion-free regions (e.g. above an accretion disk).
Icke: Many of the supercompact sources are seen to be considerably polarized. Would that not indicate that you are looking at a synchrotron source, rather tha something as exotic as you are discussing?
Svensson: Most (90%) QSOs and AGNs are radioquiet and have low polarization (<2%). These are the objects we consider. The primary energy release is likely to be nonthermal. Reprocessing is one way to 'depolarize' primary luminosity. The necessary condition, $L>10^{-3}L_{Edd}$ for pair reprocessing is not exotic. In a few highly polarized, violently varible sources we are probably looking directly at the primary energy release region.
Icke: You seem to be implying that two-photon pair creation is always the most effective process. But there is a whole class of one-photon processes $\gamma X \rightarrow X e^+ e^-$, where X completing energy-momentum conservation could be anything (ions, magnetic fields, plasma waves, whatever). Such processes could occur at much lower photon densities. Why are you excluding these?
Svensson: One-photon pair production on ions (as well as on electrons and positrons) has been considered in great detail in e.g. [35], [36]. Yes, at lower photon densities these processes are important. It turns out, however, that when plasmas become pair dominated then photon densities are almost always large enough for photon-photon interactions to dominate. B-fields of 10^{12}G necessary for magnetic one-photon pair production are somewhat too large to be tied down by accretion disks. This process may, however, play an important role in pair plasmas in γ-ray bursts.
Fischer: You have concentrated on studying the pair plasma near the active nuclei. How would your plasma interact with the accreting plasma which is presumably the source of the luminosity?
Svensson: The pairs can be created either in the (necessarily nonspherical) accretion flow or outside this flow (e.g. by photons emerging from the accretion flow). The pairs in the flow affect (1) the hydrodynamics by increasing the gas-radiation coupling, (2) the radiative transfer by increasing the opacities, and (3) the energetics (more pairs, larger cooling, lower temperatures, softer spectra). Few details have been worked out in the literature.
Singh: There are two AGNs, a Seyfert galaxy E 1615+061 and a quasar E 1821+643, which show BL Lac like steep soft X-ray spectra and no $\nu^{-0.7}$ hard X-ray spectrum, and no associated radio source. What physical processes are going on in these objects? Would not pure synchrotron mechanisms require the prescence of sufficient radio flux and the hard X-rays due to inverse Compton?
Svensson: Synchrotron self absorption easily kills the radio emission and ways of avioding high Compton fluxes are well known (e.g. relativistic beaming.
Qiu-he Peng: Is your model suitable for our Galactic Center? How do you explain the γ-ray radiation in our Galactic Center (i.e. the pair anni-

https://doi.org/10.1017/S0252921100086152 Published online by Cambridge University Press

hilation line and the higher energy continuum radiation with energy E_γ >511 keV)?
Svensson: The ℓ=4000 curve in Fig.5 fits the galactic center source fairly well implying a very compact source of $100M_\odot$ or so. The pairs would have to escape (in a wind) and annihilate on external gas at large distances to avoid gravitational redshifting.
Fischer: Can you make a physical picture of where the pair plasma is with respect to(say) the accretion disk?
Svensson: See §3.
Qiu-he Peng: Does your model consider the turbulence or some instabilities in pair plasmas? If it does, I think, some variability would occur in the luminosity of AGNs.
Svensson: Time dependent nonthermal pair production has not yet been considered but it is clear that as ℓ increases past ℓ_c rapid spectral changes will occur. See also §5.2.3 as regards instabilities. The theory of pair plasmas is presently being developed, step by step, including more and more 'well-known' micro- and macrophysics. 'Less well-known' such physics (e.g. turbulence, magnetic field effects,collective effects) introduce too many uncertainties and have less priority, at least within my thinking.
Opher: In BL Lac objects , highly polarized radiation has been observed with variability on the order of a day or less. This would imply that we are talking about compact parameters that you are talking about and that magnetic fields are imporatant and should be taken into account.
Svensson: BL Lacs are not shrouded by pair atmospheres as any reprocessing would destroy the polarization.
Opher: In the light of the BL Lac observations, if we put a dynamically important magnetic field in your compact regions, can you say (even qualitatively) the effects that can occur and that may be expected?
Svensson: The microphysics (including pair production) remain the same, while, of course, the flow geometry will change. It has often been the case in theoretical astrophysics that most of the general results of the most simple formulation of a theory will remain valid no matter how many complexities are added (see also answer to Qiu-he Peng).
Bandiera: On the basis of this model, would you expect , in the case of time variability of the source, a typical signature in the evolution of the radiation spectrum?
Svensson: The time-varying aspect of the model would first have to be specified. Rapid X-ray variability for small changes in ℓ near ℓ_c is one possibility.
Bandiera: Could collective effects,in a pair plasma, compete with the interactions with photons in determining the pair energy distribution?
Svensson: Considering the primitive nature of our knowledge of collective plasma phenomena in conditions prevailing in AGNs it is not possible to give any well-founded answer to this question (see also answer to Qiu-he Peng).